Progress In Electromagnetics Research B, Vol. 24, 131–153, 2010

ELF-EMFS INDUCED EFFECTS ON CELL LINES: CONTROLLING ELF GENERATION IN LABORATORY

M. Farina

Dipartimento di Ingegneria Biomedica, Elettronica e Telecomunicazioni
Università Politecnica delle Marche
Ancona 60131, Italy

M. Farina

MEM Research
Pescara 65010, Italy

M. A. Mariggiò and T. Pietrangelo

Dipartimento di Neuroscienze ed Imaging - CeSI
Università "G. D' Annunzio"
Chieti 66013, Italy

J. J. Stupak

Oersted Technology Corp.
24023 NE Shea Lane, Troutdale, OR 97060, USA

A. Morini

Dipartimento di Ingegneria Biomedica, Elettronica e Telecomunicazioni
Università Politecnica delle Marche
Ancona 60131, Italy

Giorgio Fanò

Dipartimento di Neuroscienze ed Imaging - CeSI
Università "G. D' Annunzio"
Chieti 66013, Italy

Received 17 June 2010, Accepted 4 August 2010, Scheduled 12 August 2010
Corresponding author: M. Farina (m.farina@univpm.it).

Abstract—The aim of this paper is to discuss the effects of the exposure to Extremely Low Frequency ElectroMagnetic Fields (ELF-EMFs) on non- and excitable cells using in vitro cell models, namely neuron-like cell line (PC12), glioblastoma-derived GL15 cells as glial model and C2C12 myocytes as muscle model, focusing our attention on standardized protocols for ELF-EMFs generation and exposure. A major issue in laboratory — and likely in nature — studies about possible biological effects of ELF waves is the difficulty in providing standard, reproducible environmental conditions. Hence, as part of the work we have developed an exposure system including a probing scanner, able to sample a given volume and to measure the time-varying magnetic field vector. The system allows detection, monitoring and removal of electromagnetic noise sources, as well as means to assess field homogeneity in terms of intensity and polarization.

1. INTRODUCTION

The biological effects of extremely low frequency electromagnetic fields (ELF-EMFs) are, to date, still an open issue attracting intensive research and resulting in a number of experimental findings, which are often controversial (see, e.g., discussion [1]). The problem has been often related to the epidemiological nature of the studies, due to the enormous number of possible factors correlating to false positives. Laboratory studies, on the other hand, have lacked, to some extent, the necessary reproducibility, because of the unavailability of commercial devices needed to provide a complete characterization of the experiments. Our present work is a laboratory study, and part of it is dedicated to design a system to check the actual exposure conditions of cells.

In living organisms, especially in vertebrates, excitable cells (neurons and muscle fibers) are more sensible to the presence of electric fields. In fact, short-time exposure (5 days) to ELF-EMF radiation saves immature primary cerebellar neurons from apoptosis and promotes survival at the flux density of 300 mT, whereas virtually no neuronal survival was observed without exposure [2]. The survival-promoting effect of ELF-EMF radiation was dependent on the size of culture flasks, suggesting that induced current plays a role in this phenomenon.

In addition, the same in vitro model, Lisi et al. described a 30% decrease of cell survival in primary rat cerebellar neurons stimulated by glutamate and exposed to 1 mT ELF-EMF waves for 5 days [3]. Other evidences came from results showing that ELF-EMF exposure

of neural progenitor cells transiently affected the transcript level of genes related to apoptosis and cell cycle control [4]. It has been found that ELF-EMF exposure for 14 days (1 h daily) increases the rate of synthesis of dopamine and serotonin in rat frontal cortex as compared to a control [5]. Using in vivo models, continuous exposure for 10 days causes a significant increase of the main antioxidant enzymatic activities in rat brain cortices.

The biological effects in cell lines exposed to ELF have been frequently noted, but the basic interaction mechanism(s) between such fields and living matter is unknown [6–8]. Several hypotheses have been suggested, but none of these has been definitely assessed by experimental data [9, 10]. It is well-known that various cellular components and processes can be affected by ELF-EMF exposure, e.g., cell membranes (both internal and external) and signal transduction pathways [11, 12], cell cycle regulation and cell proliferation and/or differentiation [13, 14]. On the other hand, direct or indirect DNA damage can also be revealed in different substrates but this does not directly lead to genotoxic effects [15, 16]. It should be mentioned that recent findings show a relationship between ELF exposure and multiple sclerosis disease [17].

In summary, the various modifications, measured in several laboratories utilizing different models, show the presence of real biological effects (acute and/or chronic) derived from ELF-EMF exposure, associated with detectable changes in cell physiology, but whose interpretation is complicated by subsequent compensatory mechanisms. For this reason we should look for an initial cellular event affected by exposure to ELF-EMFs, an event which is present in a large number of effects observed as consequences of ELF-EMF exposure.

Based on an extensive literature review, Simko and Mattsson [13] suggest that ELF-EMF exposure is able to perform such activation by means of increasing levels of free radicals. These extremely reactive molecules are ubiquitous intermediates in natural processes, and they could be the stimulus produced by ELF-EMF exposure that induces an "activated state" of the cell, which then enhances the release of free radicals, in turn leading to biological events such as those previously described [8].

The aim of our work is two fold: on one hand we describe the protocols, in particular the equipment developed to guarantee a controlled exposure of the biological models at a 50 Hz electromagnetic field, while on the other hand we report our findings about the generation of radical oxygen species (ROS) and mitochondrial membrane potential on different cellular models during "in vitro" cell

exposure to ELF-EMF radiation. The exposure is tested at different intensities and short duration (acute exposure) in pheocromocytoma-derived cell line (PC12, [18]) as neuronal models, glioblastoma-derived GL15 cells [19] as glial model and C2C12 myocytes [20] as skeletal muscle model. For the sake of the completeness it should be mentioned that the devices described for the first time in the present work, were also used on different animal and cellular models, published elsewhere and here summarized.

2. EXPOSURE SYSTEM

2.1. Design of the Radiators

The first issue in the aforementioned set of experiments was to produce a sine-wave alternating magnetic fields with 50 Hz frequency and intensity ranging from 1 μT up to 1 mT (RMS) ±2%, which was sufficiently homogeneous over a given volume and stable over time. Basically the requirement was to obtain 5% homogeneity in the volume accommodating magnetic supports for cells, a cylinder with radius 60 mm, height 190 mm for our "in vitro" cellular experiments. Incidentally, at the same time we designed radiators for "in vivo" experiments, whose biological results have already been published in [21], and where the required homogeneity was better than 5% over a much larger cylinder (diameter 710 mm and height 210 mm), a volume able to contain a plastic cage. Consequently the measurement system, reported in the next section, was designed and tested to perform measurements over larger volumes with the same accuracy.

For radiators, we have selected and designed two classes of coils, namely Helmholtz coils and cylindrical solenoids. Helmholtz coils were designed to radiate cells while under the confocal microscope, as well as to radiate mice for experiments reported in [21], while solenoids were used in the incubators to test longer exposures. Helmholtz coils are useful for producing a very uniform magnetic field within a test region, while also allowing unobstructed access to the test region from every side. There is an axial spacing for which the second derivative of the magnetic field contribution from each coil vanishes, as does, of course, the second derivative of the summed field of two coils. This vanishing of the second derivative is sometimes called the Helmholtz criterion. For standard round coils, it occurs at a coil spacing from the centerlines of the coil cross-sections of one half coil radius. However, coils of square rather than round shape (on their major dimensions) may be used and have advantages for certain purposes. The space inside the coils in which the field is sufficiently uniform to meet the requirements of the work may be called the useful volume. The useful

volume of a round coil set is round with approximately flat ends, that is pillbox shaped. The useful volume of a square Helmholtz coil set, by comparison, is more rectangular. This shape was chosen for the Helmholtz coil sets discussed here.

The coil spacing needed to meet the Helmholtz criterion for square coils is:

$$w = 0.54450564\,\mathrm{s} \tag{1}$$

where w is the axial spacing between coils (measured from the coil centerlines) and s is the side length (between coil centerlines).

With this spacing, the coil constant, that is the magnetic flux density per ampere at the center, is:

$$B_z = \frac{1.2961\mu_0 ni}{s} \tag{2}$$

The fields of square Helmholtz coils are less accurately predicted by calculations than round ones because the conducting wires of the coils bend sharply at the corners but not in the middle of the spans, and so are difficult to locate accurately. In any case, the field produced at the center of a Helmholtz coil is exactly determined by the current, number of turns, and coil geometry: the error in the magnetic field will be an issue of accuracy in the coil realization. In this work, the square coils had errors of less than one percent, as built, both individually and as a set.

When the coils are assembled, the coil constant is checked by use of a gaussmeter of sufficient accuracy, in recent calibration, measuring the magnetic field at the coil center. This reading is divided by the current in the coils to obtain the coil constant, expressible in units of gauss per ampere or Tesla per ampere. The accuracy of such a measurement depends on the accuracy of the current measurement (which in this case was accurate to over six places), and the accuracy of the gaussmeter and its Hall-effect probe. The overall accuracy of this measurement was believed to be within 0.25%. Data for the Helmholtz coils are reported in Table 1.

In addition to these two high-accuracy Helmholtz coils, two cylindrical coils were built, with thin walls and of length longer than the diameter. These coils have much larger surface area to winding volume ratios than can be achieved with Helmholtz coils. They are capable of producing higher fields and provide greater power dissipation, allowing these fields to be maintained for longer periods of time, but at the cost of reduced magnetic field homogeneity. Such coils were developed to irradiate cells when in the incubator. For a uniformly wound thin-

Table 1. Parameters for Helmholtz coils.

Application	Side length [mm]	Axial separation [mm]	Coil constant at the center [G/A]	Number of wire turns (per coil)	Resistance at 20 °C [Ω]
Radiation of mice [21]	1396	760	1.075	94 (AWG 10)	3.35
Radiation of cells under microscope	828	451	1.26	64 (AWG 12)	2.21

walled solenoidal coil, the field on the axis is well-known to be:

$$B_z = \frac{\mu_0 n\, i r^2}{2\ (z^2 + r^2)^{3/2}} \tag{3}$$

A coil of this type has a field which is strongest at the center (compared to other measurements made on the axis), and drops to roughly half that at the coil ends. In order to improve the homogeneity, however, these coils were wound with varying turns per length, and the resulting fields thus vary in a manner which was best analyzed using a computer (finite-element) program. Parameters for such coils are reported in Table 2.

In particular, a first vertical solenoid was set on a carrier and put on a supporting base, both made of bakelite nonmagnetic material, with maximal thermal and mechanical stability suitable for long term operations. A plastic nonmagnetic support was used to place broth-culture contained in glass flask transparent to the ELF magnetic field. The solenoid was vertically built to facilitate broth cultures incubation and placed into an incubator (Heraeus 5042E, Hamburg, Germany) at a constant monitored temperature of 37.8C. In this case, 188 of the total 212 turns were wound in a single inside layer over the entire length, and an additional 12 turns were wound in a second partial layer over each end to a length of 30 mm.

A second, horizontal, solenoid was designed to radiate a larger number of cells, still in incubator. In this case, of a total of 144 turns, 120 turns were wound evenly in a single layer over the length, and an additional 12 turns were wound in a second, outside partial layer over each end to a length of 30 mm.

Care was used to keep power dissipated in the coils as low as

Table 2. Parameters for solenoids.

Application	Diameter [mm]	Length [mm]	Coil constant at the center [G/A]	Number of wire turns (per coil)	Resistance at 20 °C [Ω]
Radiation of broth-cultures in incubator	176	450	4.98	212 (AWG 13)	0.78
Radiation of large number of cells in incubator	124	300	4.83	144 (AWG 13)	0.3

possible, so as to avoid any significant change in the environmental temperature. Nonetheless, temperature was recorded during the experiments.

In order to guarantee stability over time, AC (alternating-current) power supplies fed field-generating coils in current closed-loop mode of operation; the power supplies were by Elgar (Elgar, San Diego, CA), CW series, featuring an internal feedback sense system. In particular, depending on the currents needed, two models were used: CW-1251P and CW-801P.

2.2. Design of the Vector Measurement System

Aim of this section is to describe how we have designed and realized a mechanically scanned system, able to perform a point-by-point measurement of the low-frequency vector magnetic field.

The vector measurement system was designed to test the actual field homogeneity in the actual operating environment. In fact, while it is obvious that coils will outperform specifications in an ideal empty environment, the fields have to be tested when surrounding metal masses and instruments are present. The maximum scanning volume is $65 \times 32 \times 14\,\mathrm{cm}^3$ and the maximum spatial resolution is around $200\,\mu\mathrm{m}$: the device was designed to be able to sample the large cage volume used in [21] and at the same time the small areas in solenoids for the incubator. In order to reduce the impact of the mechanical part of the measurement systems, they were constructed with plastic

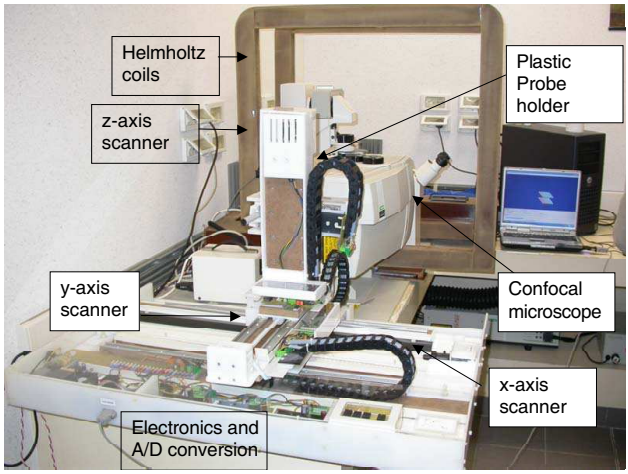

Figure 1. Image of the 3D vector measurement system, while being tested with the smaller version of Helmholtz coils, designed to be adapted to a confocal microscope and to produce electromagnetic fields centered on the observed cell samples.

materials, mostly in-house: a picture of the final device is Figure 1: step motors attached to worm-screws allow a precise control over the three spatial axes. A magnetic sensor, a thri-axial magnetoresistive sensor HMC2003 by Honeywell, is mounted at the end of a plastic bar, keeping electronics and motors far enough from the measurement volume; the plastic bar also allowed measurement inside the solenoid coils. The magnetoresistive sensor was selected owing to its inherently higher sensitivity- if compared, e.g., to Hall sensors-, complying with the requirement of detecting low intensity magnetic fields. It features a measurement capability between 4 nT and 0.2 mT with a linearity of 1%, resolution of 4 nT and temperature variation of 600 ppm/C°. Its bandwidth is 1 kHz. Note that 0.2 mT is less than the 1 mT that was planned for part of the experiment, but the scanning system was introduced to measure field homogeneity and not the absolute field intensity. The latter is in fact measured independently by using a standard F. W. BELL Tesla meters mod. 4190 (measuring range: 0.01–200 mT, resolution: 0.01 mT) and mod. 6010 equipped with an axial probe mod. HAD61-2508-05T (measuring range: 0.3–300 mT, minimum resolution: 0.01 mT) both from Sypris Test & Measurement (Orlando, FL).

Hence, the homogeneity of the field is tested by selecting the current in order to produce a maximum magnetic field of 0.2 mT.

Of course that, the system is used to verify that the homogeneity is satisfactory in the working area when the experimental setup is complete.

The plastic bar is driven along the three axes in order to map the field across the volume by means of stepped motors. Stepped motors are only powered for the time needed to displace the sensor, and nearly all electronics are switched off during magnetic field sampling in order to reduce magnetic disturbance of the measuring system itself.

An internal magnetic field can be generated across the sensor, providing the possibility of calibrating out unwanted magnetic fields. This also allows the sensor "zero" to be shifted, in order to avoid a lower sensor saturation level in presence of static magnetic fields (including the Earth's magnetic field). The internal coil is controlled by an A/D converter. The output from the sensor is sampled converted to a 12-bit digital word, and sent to a PC via RS-232 X. Sampling rate and sensor features allow to process incoming signals up to 1 kHz. A "PIC" microcontroller from Microchip handles the stepping motors, the data coming from the sensor and the PC program, as shown in Figure 2.

The sensor is calibrated by producing a magnetic field with a solenoid and comparing data recorded at a fixed point by our instrument and a standard calibrated gaussmeter.

Data in the PC are processed by means of an FFT algorithm to determine the spectral content of the incoming signal. In order to preserve phase information of the magnetic field during the volume

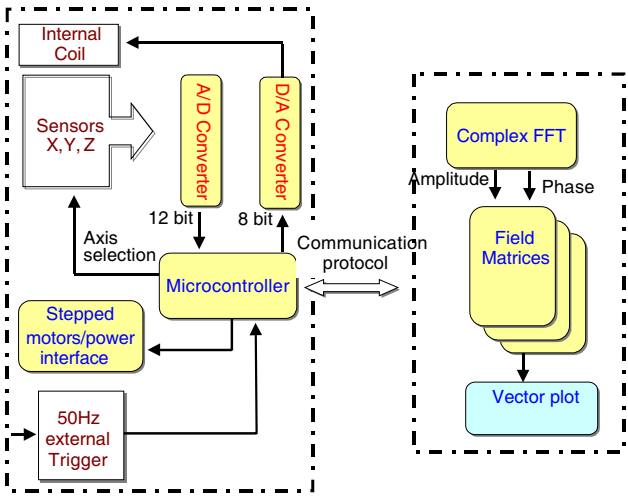

Figure 2. Block diagram of the system.

scan, an external triggering signal is obtained directly from the generator, so that sampled data are synchronized with the field generator. At the end of the scanning process, for each point of the space volume there are — for each spectral component — three complex measurements available, one for each axis. At a given instant t_0, the plotted magnetic vector is

$$\mathbf{B}\,(x, y, z, t) = \mathrm{Re}\left(\tilde{\mathbf{B}}_n\,(x, y, z)\, e^{j\omega_n t_0}\right) \tag{4}$$

where $\tilde{\mathbf{B}}_n$ is the n-th complex harmonic resulting from the FFT, and ω_n is the corresponding angular frequency. This way one obtains a "picture" of the spatial magnetic field distribution — for a certain frequency — at time t_0 with respect to the synchronization signal. Such a data is useful, as it allows the experimenter to record and check field homogeneity in terms of *polarization*, not only intensity.

When measurements have to be performed over fields featuring small intensities, close to the noise ground, a simple calibration routine is adopted. A first scan is performed while the generator is switched off, and results of FFT analysis of the measurements are stored in memory. Those data represent the "environmental" disturbances, coming from sources commonly present in a laboratory. Hence, after a second scan with the generator on, the harmonic-by-harmonic difference is plotted.

The coils used in these experiments were built by Oersted Technology Inc. (Troutdale, OR) according to what described in the previous section, and fully characterized. Measurements were then performed on the coils involved in the experiment "in situ" (namely with the solenoids in the incubators, the big Helmholtz coils with the cage inside).

They confirmed that field homogeneity was always in the desired range, in spite of the presence of several metal objects in proximity of the coils, which added a disturbance due to eddy currents flowing within the conductors. Figure 3 shows the field measured in proximity of a circular coil, clearly a low homogeneity coil that is reported only to highlight one of the outputs of the software that we have developed in this framework, directly in vector format. In this case the image is qualitative, but individual plane sections are checked to verify the actual working conditions. This is done for example in Figure 4, showing a quantitative plot of the magnetic field in the working XY plane for the larger Helmholtz coil set after settling to a nominal effective value of 0.1 mT: in all planes the magnetic field was confirmed to be within 5% of the nominal value in spite of disturbances caused by nearby instruments.

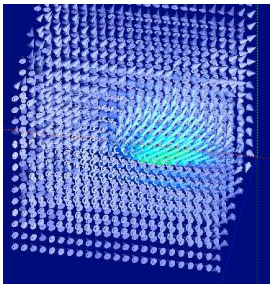

Figure 3. Example of magnetic field vector plot; the magnetic field is generated by a coil.

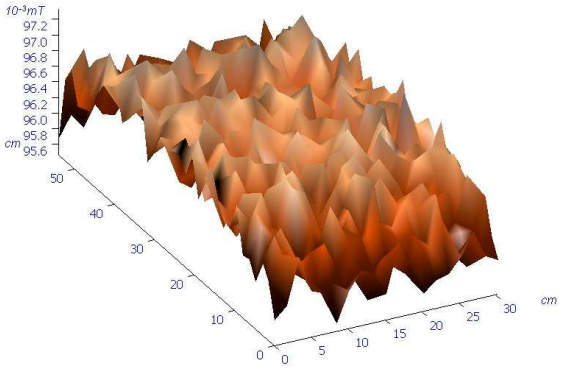

Figure 4. Effective magnetic field recorded in the working area of the bigger Helmholtz coils when 0.1 mT is being radiated. The field is homogeneous with an intensity of about 0.096 mT.

3. BIOLOGICAL STUDIES

In order to check the biological effects of the ELF-EMFs generated by the solenoids and the Helmholtz coils, different experimental models were used.

In this section, we reference published results (animal models and cellular model with prokariotic cells) and report new results (eukariotic cells) so as to provide a complete scenario; in all cases the biological systems were exposed by using the devices described in the previous section.

A preliminary measurement of the background electromagnetic fields was performed: in the laboratories it was less than 1 microT (50 Hz). In particular it was in the order of 0.7 microT (50 Hz) in the incubator outside the ELF radiators, when the latter were switched "on" and radiating at the higher intensity of 1 mT, and of 100 nT (50 Hz) outside or inside the switched off devices placed in the incubator.

The radiation parameters chosen in the studies described below (0.1, 0.5 and 1.0 mT; 50 Hz), were selected since they reflect the both common and limit exposure in urban environments and in domestic appliances.

3.1. Animal Models

Two animal models were exposed to ELF-EMFs using the big Helmholtz coils. Using our experimental equipment, Falone et al. [22] showed that when female Sprague-Dawley rats were continuously exposed to a sinusoidal 50 Hz 0.1 mT magnetic field for 10 days, some changes in the major antioxidant systems of the brain and in the neurotrophic support were observed depending on the animal age. In fact, exposed young rats enhanced their neurotrophic signaling and anti-oxidative enzymatic defense, while aged animals underwent a significant decrease in the major antioxidant enzymatic activities.

The research group of Prof Musiani exposed young and adult wild type and transgenic mice representing a model of HER-2-dependent mammary carcinogenesis [21] to ELF-EMFs, produced by the big Helmholtz coils. They revealed that in 1mT exposed young, but not in adult, wild type mice there was a transient decrease of body weight and a decrease in bone marrow and splenic myelopoietic cells, whereas there were no hematological differences between treated and control transgenic mice. In addition it appeared that ELF-EMFs do not influence mammary carcinogenesis.

Once more these results showed that ELF-EMFs produce a biological stress that can be faced and counteracted.

3.2. Cellular Models

3.2.1. Prokariotic Cells

A vertical solenoid in an incubator was used to expose the bacterium Escherichia coli to 0.1–1.0 mT ELF-EMFs. Under these conditions, Cellini et al. [23] showed that exposed samples and controls displayed similar total and cultivable cell numbers, while in the exposed populations atypical lengthened bacterial forms were observed suggesting a probable alteration during cell division. These results indicated that exposure to 50 Hz EMF acts as a stressing factor on bacteria even if it did not alter their ability to proliferate.

3.2.2. Eukariotic Cells

To complete the panel of the experimental approaches and to determine if the "in vitro" cell exposure to ELF-EMFs influences cell biology, we performed new pilot experiments using in vitro cell models of non- and excitable cells, namely neuron-like cell line (PC12), glioblastoma GL15 as glial model and C2C12 myocytes as skeletal muscle model. These cell lines were exposed to 0.1–1.0 mT ELF-EMFs for different times to

simulate acute (minutes) and chronic (7 days, equivalent to about 3 duplication cycles) exposures.

Numerous previous studies reported that the cellular oxidative machinery was targeted during ELF-EMFs exposure [13, 24, 25]. For this reason, during acute exposure the production of reactive oxygen species (ROS) and the mitochondrial membrane variations were monitored using specific fluorescent probes and the confocal microscope equipped with a pair of Helmholtz coils, as above described.

In particular ROS production was assayed loading the cells with the DCFH2 probe, whose fluorescence increase is indicative of ROS production. The probe fluorescence emission was recorded every 30 s for a total observation period of 30 min in the absence (the coils were switched off) or presence of ELF-EMFs (the coils were switched on). Representative images of this experimental approach are shown in Figure 5(a).

After cell fluorescence recordings, the quantitative analyses regarding the kinetic fluorescence emission versus time and the number of cells revealing fluorescence increase (namely "activated cells") were performed. These results indicated that each cell line showed a specific behavior in the presence of ELF-EMFs also depending on the field intensity. The graph presented in Figure 5(b) depicts the fluorescence variations to time in PC12 and GL15 "activated cells" revealing different kinetics and consequently different cell reactivity in the presence of EM radiation. ELF-EMF exposure induced in PC12 cells a slight increase in the number of cells showing higher fluorescence

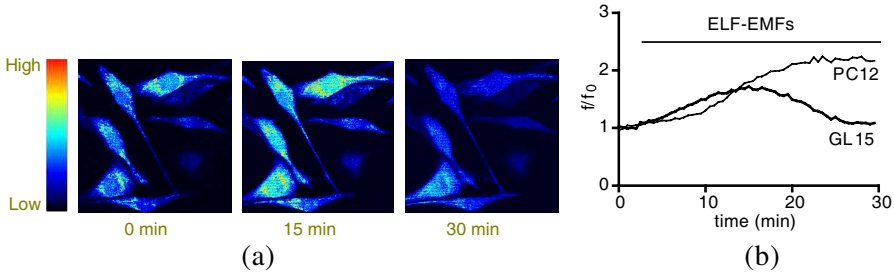

Figure 5. (a) Sample images in pseudocolours acquired at the indicated times in an experiment analyzing the ELF-EMF-induced ROS on GL15 cells. The pseudocolors indicated show the fluorescence interval: from black to red representing from low to high fluorescence levels, respectively, and therefore the same for ROS. $n = 10$. (b) Temporal analyses of the fluorescence (f/f_0) of single PC12 or GL 15 cells. Each trace is representative of the behavior of a single cell.

and consequently producing ROS depending on the intensity of the field used. In fact the "active cells" were about 10% (total number of tested cells was 47) in the non exposed population and increased to 20% (total number of tested cells was 51) and 35% (total number of tested cells was 45) cell population exposed to 0.1 mT and 1.0 mT, respectively. Even if at a lower extent, also GL15 cells showed a similar behavior. In contrast, the C2C12 cells did not show a clear reproducible response; apparently there were no significantly different responses between non exposed controls and 0.1 mT exposed C2C12 cells, and the exposure to 1.0 mT induced a bleaching effect on the fluorescent probe.

The variation in the mitochondrial potential is another parameter that was analyzed as an index of oxidative stress. This fluorescence analysis was performed using molecule JC-1 as a fluorescent probe under the same experimental conditions and with the same set-up used for the analysis of the ROS production. In particular, JC-1 has a peculiar double emission when excited at 488 nm: it is seen in a monomeric form emitting green fluorescence (λ 529 nm) or in the "J-aggregate" form with a red fluorescence (λ 590 nm). The green and red emission of this molecule is a function of the mitochondrial membrane polarization. In the presence of a high mitochondrial potential, the dye tends to the J-aggregate, emitting in the red, conversely low mitochondrial potential induced monomers formation and green emission. This latter condition is often considered the consequence of an oxidative stress status. Figures 6(a) shows

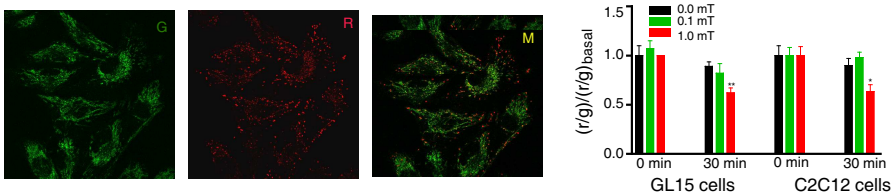

(a) (b)

Figure 6. (a) Images acquired during the analysis of the mitochondrial membrane potential in GL15 cells exposed to ELF-EMF. The images were acquired simultaneously in the green (**G**) and red (**R**), with their digital merge in **M**. Scale bar: 10 µm. (b) Mitochondrial potential variations in GL15 and C2C12 cells after 30 min exposure to 0.0, 0.1 and 1.0 mT ELF-EMFs. The data are means ± Standard Error of the Mean (SEM); test statistics: $n = 10$. * $p < 0.05$ and ** $p < 0.01$ vs each 0.0 mT representing non exposed control cells.

representative images that were acquired during the monitoring of the mitochondrial membrane potential in GL15 cells exposed to the ELF-EMFs.

From these images, changes concerning the behavior of the probe as a function of the mitochondrial potential are hardly seen, and for this reason a quantitative analysis was carried out utilizing software for image analysis. For each cell field examined, the ratio between the fluorescence in the red and that of the green channel (r/g) was determined and normalized according to the mean values of the ratio of the same basal fluorescences (r/g basal); these changes were followed as a function of time. These analyses revealed that exposure to ELF-EMFs of 1.0 mT significantly decreased the mitochondrial potential both in GL15 and C2C12 cells (Figure 6(b)). The data concerning PC12 cells did not reveal any clear and significant relationship between mitochondrial potential and the presence of ELF-EMFs.

Even with different responses, the tested cell lines revealed a sensitivity to the presence of the electromagnetic radiation. To test if the acute responses induced persistent biological effects and/or if they depended on the exposure times, the PC12, GL15 and C2C12 cells were continuously exposed for 7 days to ELF-EMFs.

Chronic exposure up to 1.0 mT ELF-EMF intensities did not revealed significant modifications in cell morphology, proliferation rate and differentiation marker expression. Figure 7 collects sampled photos of proliferating control or ELF-EMF-exposed cells that showed similar

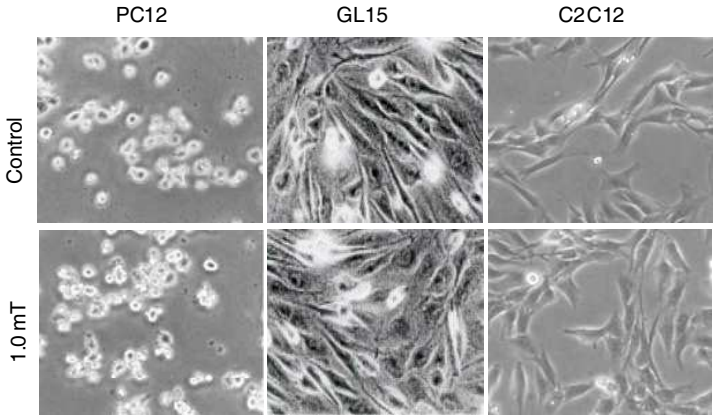

Figure 7. Images acquired in bright field of non-differentiated PC12, GL15 and C2C12 cells, grown for seven days in the absence (Control) and presence of ELF-EMFs at an intensity of 1.0 mT, as indicated.

Table 3. Cell proliferation of three cell lines (PC12, GL15 and C2C12) after 7 day exposure to ELF-EMF of different intensities (0.1, 0.5 and 1.0 mT). Cells were plated (30×103/dish) at time 0 and after 7 days culturing in absence or presence of elf the cell number was assayed using a Burker chamber slide under a transmitted light optical microscope (LEICA DMIL).

Proliferating cells (mean of the cell number/1000 ± SEM days in growth medium, $n = 5$)				
	Control	0.1 mT	0.5 mT	1.0 mT
PC12	108.0 ± 6.2	101.0 ± 7.1	105.0 ± 5.2	102.0 ± 5.3
GL15	118.0 ± 7.2	121.0 ± 6.5	119.2 ± 6.7	122.3 ± 6.3
C2C12	161.3 ± 14.6	174.7 ± 18.8	199.5 ± 18.8	159.5 ± 26.8

cell morphology.

The proliferation rate of these cells was not influenced by the presence of ELF-EMFs. In fact, after seven day exposure to 0.1, 0.5 or 1.0 mT ELF-EMFs the number of proliferating cells was comparable to that present in control populations as reported in Table 3.

The differentiation process of these cell lines was performed during ELF-EMF exposure. In absence or presence of 1.0 mT ELF-EMFs, PC2 cells were differentiated towards the neuroadrenergic phenotype for 7 days in presence of 50 ng/ml NGF, a specific neuronal growth factor, GL15 and C2C12 were differentiated for 7 days in presence of low serum medium towards the astrocytic and skeletal muscle phenotypes respectively. After these treatments PC12, GL15 and C2C12 cells were fixed and immunolabelled for specific differentiation markers. In particular PC12 were immunolabelled for neuronal "enolase", a neuronal specific enzyme [26], GL15 for GFAP a specific component of astrocyte cytoskeleton [19], and C2C12 for MF20 as specific protein for the skeletal muscle phenotype [27]. As shown in the photo gallery presented in Figure 8, the presence of ELF-EMFs during cell differentiation did not significantly modify the specific markers distribution in each phenotype.

3.3. Discussion

The effects of ELF-EMFs depended on their intensity and time exposure. In addition, the cell response was related to the cell phenotype. Even if further studies remain necessary to identify the oxidative stress pathway induced and/or the specific ROS produced by the exposure to ELF-EMF, we propose the biochemical pattern related to the oxidative status as the candidate for the cellular "primum

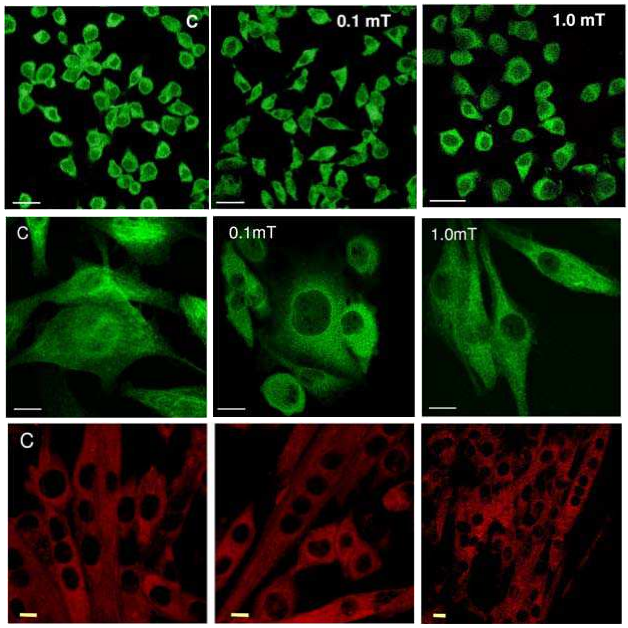

Figure 8. (Top) PC12 cells differentiated in the presence of NGF for seven days in the absence (C) and presence of exposure to ELF-EMF at intensities of 0.1 mT and 1.0 mT. The fluorescence signal and intensity revealed that the enzyme localization was present in the soma of the cells in all tested conditions. The cells were labeled to reveal the localisation of enolase with an antibody labeled with Alexa488. Scale bar: 20 µm. (Middle) GL15 cells differentiated for seven days in low serum in the absence (C) and presence of exposure to ELF-EMF at intensities of 0.1 mT and 1.0 mT. The cells were labeled to reveal the localisation of GFAP with an antibody labelled with Alexa488. Scale bar: 20 µm. (Bottom) C2C12 cells differentiated for seven days with low serum in the absence (C) and presence of exposure to ELF-EMF at intensities of 0.1 mT and 1.0 mT. The cells were labeled to reveal the expression of the protein MF20 with an antibody labeled with Alexa562. Scale bar: 10 µm.

movens" of ELF-EMF-induced effects on biological systems.

In our experimental conditions, ELF-EMF affected the oxidative status, but the cells counteracted the induced increase of ROS production or decrease of mitochondrial membrane potential probably modifying their antioxidant ability [28]. The lack of a cytotoxic or transforming effect exerted by the radiation, was confirmed by the

fact that cell morphology, proliferation and differentiation were not modified after long time exposure to ELF-EMFs up to 1.0 mT.

As previously demonstrated by Ross in the 90's [29], markedly different effects, ranging from inhibition to stimulation of proliferation, were obtained, depending on the signal parameters (amplitude and frequency of ELF-EMF) as well as the types of utilized cell substrate. This fact is also supported by somewhat unclear results on the effect of the ELF-EMF on stromal stem cell proliferation (colony forming unit of fibroblast, CFU-f); in fact, CFU-f from female mice showed a reduction, while CFU-f from male mice no decrease in cell proliferation [30].

More recently Wolf et al. [31] showed that the stimulation of proliferation, as well as the presence of DNA damage, was noted in HL-60 leukemia cells, Rat-1 fibroblasts and WI-38 diploid fibroblasts exposed for 24–72 h to 0.5–1.0-mT ELF-EMF. These effects were prevented by pre-treatment of cells with an antioxidant like alpha-tocopherol, suggesting that redox reactions were involved. Accordingly, in our experiments the cells after exposure to 1.0 mT ELF-EMF exhibited a significant increase in ROS accumulation which was decreased by addition in the culture medium of an adequate scavenger. Under our experimental conditions it was also possible to note a significant increase of ROS production in two tested cell lines even with a different qualitative and quantitative time-course. It should be mentioned that "in vivo" experiments in literature also seem to confirm that chronic exposure to ELF-EMF is able to generate a stress oxidative status [32–34]. The "in vitro" experiments reported here, as well as the results derived from "in vivo" techniques [13, 22, 24, 25, 28, 35, 36] in mice, show that the presence of ELF-EMF can induce a variable and specie-specific alteration of the stress oxidative pathway.

4. CONCLUSION

In our study, different approaches were used to face the question regarding the biological effects of ELF-EMF. The functional link between the presence of electromagnetic fields and modifications to physiological and/or pathological processes in living organisms, including man, has been known for a long time and used even in therapy. The scientific basis of these effects and their mechanisms of action, which might explain the relationships between EMFs and their biological effects on living matter, are still far from being known. For these reasons a lot of groups are involved in this research field, and often the EMF-generating devices were broadly used in the laboratories

without checking their settings. These considerations invited us to plan this study mainly structured in two parts: the technological and biological ones.

The first aim was to design specific EMF-generating devices in order to satisfy the requirements of biologists (volumes exposure for animals or cells, accessibility, easy handling, device positioning in incubator or microscope, etc.) and ensure properly device settings.

The second goal was to check if the assembly devices really generate the required field in the laboratories. To this aim, we designed and built a volumetric mapping system able to measure, filter and plot time-varying (ELF) vector magnetic field in a prescribed area. Even a similar device has recently been proposed for mapping static fields of large magnets in high energy accelerators [37], there are several differences between the system described by Hirose et al. [37] and the one proposed here. In addition, while Hirose group [37] conceived a device for static intense fields (and consequently used Hall sensors), our device exploited magnetoresistive sensors along with a time-sampling device and an FFT algorithm, in order to also detect small-intensity time-varying fields.

As mentioned above, these devices were used to study ELF-EMF induced effects on different models, from animals to cells. The last one was the model on which we focused our attention in particular because, using the Helmholtz coils put on the confocal microscope, we were able to check the cellular response during the exposure.

We have analysed the effects of ELF (50 Hz) on neuron-like cell line (PC12), glioblastoma GL15 as glial model and C2C12 myocytes as muscle model, focusing our attention on the cellular oxidative stress machinery.

As the result of the exposure, PC12, GL15 and C2C12 seem to indicate that the acute response (ROS production and/or mitochondrial membrane potential decrease) to ELF-EMF (0.1–1.0 mT) exposure strictly depends on cell model rather than on the utilized ELF-EMF intensity or time of exposure. In both neuronal-like and glial-like cell lines, however, a significant increase of ROS production was detected, with a different time-course in each cell line. In GL15 cells, this probably caused the decrease of mitochondrial membrane potential also observed in C2C12 cells. Thus the ELF-EMF-induced biological effect could be detected in the perturbation of the oxidative status that the cell can counteract depending on its phenotype.

ACKNOWLEDGMENT

The authors are grateful to Dr. Nickolay C. Iliev for his contribution in developing the specifications of the coils used in the experiments. Moreover, the authors would like to thank Ing. Andrea Pietrangelo for performing the field homogeneity measurements.

REFERENCES

1. Coen, R. L., "Don't be shocked, power lines are safe!," *IEEE Spectrum*, Vol. 37, No. 9, 22, 2000.
2. Odaa, T. and T. Koike, "Magnetic field exposure saves rat cerebellar granule neurons from apoptosis in vitro," *Neuroscience Lett.*, Vol. 365, 83–86, 2004.
3. Lisi, A., et al., "Exposure to 50 Hz electromagnetic radiation promote early maturation and differentiation in newborn rat cerebellar granule neurons," *J. Cell Physiol.*, Vol. 204, No. 2, 532–538, 2005.
4. Nikolova, T., et al., "Electromagnetic fields affect transcript levels of apoptosis-related genes in embryonic stem cell-derived neural progenitor cells," *FASEB J.*, Vol. 19, No. 12, 1686–1688, 2005.
5. Sieron, A., et al., "Alternating extremely low frequency magnetic field increases turnover of dopamine and serotonin in rat frontal cortex," *Bioelectromagnetics*, Vol. 25, No. 6, 426–430, 2004.
6. Kavet, R., M. A. Stuchly, W. H. Bailey, and T. D. Bracken, "Evaluation of biological effects, dosimetric models, and exposure assessment related to ELF electric- and magnetic-field guidelines," *Appl. Occup. Environ. Hyg.*, Vol. 16, No. 12, 1118–1138, 2001.
7. Foster, K. R., "Mechanisms of interaction of extremely low frequency electric fields and biological systems," *Radiat. Prot. Dosimetry*, Vol. 106, No. 4, 301–310, 2003.
8. Santini, M. T., et al., "Cellular effects of extremely low frequency (ELF) electromagnetic fields," *Int. J. Radiat. Biol.*, Vol. 85, No. 4, 294–313, 2009.
9. Repacholi, M. H., "WHO's health risk assessment of ELF fields," *Radiat. Prot. Dosimetry*, Vol. 106, No. 4, 297–299, 2003.
10. Preece, A. W., J. W. Hand, R. N. Clarke, and A. Stewart, "Power frequency electromagnetic fields and health. Where's the evidence?" *Phys. Med. Biol.*, Vol. 45, No. 9, 139–154, 2000.
11. Piacentini, R., et al., "Extremely low-frequency electromagnetic fields promote in vitro neurogenesis via upregulation of Ca(v)1-channel activity," *J. Cell. Physiol.* Vol. 215, 129–139, 2008.

12. Czyz, J., T. Nikolova, J. Schuderer, N. Kuster, and A. M. Wobus, "Non-thermal effects of power-line magnetic fields (50 Hz) on gene expression levels of pluripotent embryonic stem cells-the role of tumour suppressor p53," *Mutat. Res.*, Vol. 557, No. 1, 63–74, 2004.
13. Simko, M. and M. O. Mattsson, "Extremely low frequency electromagnetic fields as effectors of cellular responses in vitro: Possible immune cell activation," *J. Cell Biochem.*, Vol. 93, No. 1, 83–92, 2004.
14. Frahm, J., M. Lantow, M. Lupke, D. G. Weiss, and M. Simko, "Alteration in cellular functions in mouse macrophages after exposure to 50 Hz magnetic fields," *J. Cell. Biochem.*, Vol. 99, No. 1, 168–177, 2006.
15. Villarini, M., M. Moretti, G. Scassellati-Sforzolini, B. Boccioli, and R. Pasquini, "Effects of co-exposure to extremely low frequency (50 Hz) magnetic fields and xenobiotics determined in vitro by the alkaline comet assay," *Sci. Total Environ.*, Vol. 361, No. 1–3, 208–219, 2006.
16. Stronati, L., A. Testa, P. Villani, C. Marino, G. A. Lovisolo, D. Conti, F. Russo, A. M. Fresegna, and E. Cordelli, "Absence of genotoxicity in human blood cells exposed to 50 Hz magnetic fields as assessed by comet assay, chromosome aberration, micronucleus, and sister chromatid exchange analyses," *Bioelectromagnetics*, Vol. 25, No. 1, 41–48, 2004.
17. Canbay, C., "The essential environmental cause of multiple sclerosis disease," *Progress In Electromagnetics Research*, Vol. 101, 375–391, 2010.
18. Greene, L. A. and A. S. Tischler, "Establishment of a noradrenergic clonal line of rat adrenal pheochromocytoma cells which respond to nerve growth factor," *Proceedings of the National Academy of Sciences of the United States of America*, Vol. 73, 2424–2428, 1976.
19. Mariggiò, M. A., G. Mazzoleni, T. Pietrangelo, S. Guarnieri, C. Morabito, N. Steimberg, and G. Fanò, "Calcium-mediated transductive systems and functionally active gap junctions in astrocyte-like GL15 cells," *BMC Physiology*, Vol. 1, 4, 2001.
20. Yaffe, D. and O. Saxel, "Serial passaging and differentiation of myogenic cells isolated from dystrophic mouse muscle," *Nature*, Vol. 270, 725–727, 1977.
21. Iezzi, M., P. Felicetti, L. Borgia, T. Pannellini, G. Fanò, M. A. Mariggio, A. Pietrangelo, A. Mezzetti, F. Cuccurullo, and P. Musiani, "Effects of ELF-EMF exposure on haemopoiesis and mammary carcinogenesis in BALB/c mice," *Biological Effects of*

Electromagnetic Fields, Kostarakis(ed.), Vol. 1, 57–65, 2006.

22. Falone, S., et al., "Chronic exposure to 50 Hz magnetic fields causes a significant weakening of antioxidant defence systems in aged rat brain," *Int. J. Biochem. Cell. Biol.*, Vol. 40, No. 12, 2762–2770, 2008.
23. Cellini, L., et al., "Bacterial response to the exposure of 50 Hz electromagnetic fields," *Bioelectromagnetics*, Vol. 29, No. 4, 302–311, 2008.
24. Falone, S., et al., "Fifty hertz extremely low-frequency electromagnetic field causes changes in redox and differentiative status in neuroblastoma cells," *Int. J. Biochem. Cell. Biol.*, Vol. 39, No. 11, 2093–2106, 2007.
25. Di Loreto, S., et al., "Fifty hertz extremely low-frequency magnetic field exposure elicits redox and trophic response in rat-cortical neurons," *J. Cell. Physiol.*, Vol. 219, No. 2, 334–343, 2009.
26. Anand, N. and L. G. Stead, "Neuron-specific enolase as a marker for acute ischemic stroke: A systematic review," *Cerebrovasc Dis.*, Vol. 20, No. 4, 213–219, 2005.
27. Pietrangelo, T., et al., "Extracellular guanosine-5'triphosphate modulates myogenesis via intermediate Ca2+-activated K+ currents on C2C12 mouse cells," *J. Physiol.*, Vol. 572, Pt. 3, 721–733, 2006.
28. Mariggiò, M. A., et al., "Extremely low frequency electromagnetic fields and oxidative stress in excitable cell lines," *Biological Effects of Electromagnetic Fields*, Kostarakis (ed.), Vol. 2, 1043–1050, 2006.
29. Ross, S. M., "Combined DC and ELF magnetic fields can alter cell proliferation," *Bioelectromagnetics*, Vol. 15, No. 5, 493, 1994.
30. Van Den Heuvel, R., H. Leppens, G. Nemethova, and L. Verschaeve, "Haemopoietic cell proliferation in murine bone marrow cells exposed to extreme low frequency (ELF) electromagnetic fields," *Toxicol in Vitro*, Vol. 15, No. 4–5, 351–355, 2001.
31. Wolf, F. I., et al., "50-Hz extremely low frequency electromagnetic fields enhance cell proliferation and DNA damage: Possible involvement of a redox mechanism," *Biochim. Biophys. Acta.*, Vol. 1743, No. 1–2, 120–129, 2005.
32. Regoli, F., S. Gorbi, N. Machella, S. Tedesco, M. Benedetti, R. Bocchetti, A. Notti, D. Fattorini, F. Piva, and G. Principato, "Pro-oxidant effects of extremely low frequency electromagnetic fields in the land snail Helix aspersa," *Free Radic. Biol. Med.*,

Vol. 39, No. 12, 1620–1628, 2005.

33. Harakawa, S., N. Inoue, T. Hori, K. Tochio, T. Kariya, K. Takahashi, F. Doge, H. Suzuki, and H. Nagasawa, "Effects of a 50 Hz electric field on plasma lipid peroxide level and antioxidant activity in rats," *Bioelectromagnetics*, Vol. 26, No. 7, 589–594, 2005.
34. Yokus, B., D. U. Cakir, M. Z. Akdag, C. Sert, and N. Mete, "Oxidative DNA damage in rats exposed to extremely low frequency electro magnetic fields," *Free Radic Res.*, Vol. 39, No. 3, 317–323, 2005.
35. Lee, B. C., H. M. Johng, J. K. Lim, J. H. Jeong, K. Y. Baik, T. J. Nam, J. H. Lee, J. Kim, U. D. Sohn, G. Yoon, S. Shin, and K. S. Soh, "Effects of extremely low frequency magnetic field on the antioxidant defense system in mouse brain: A chemiluminescence study," *J. Photochem. Photobiol. B*, Vol. 73, No. 1–2, 43–48, 2004.
36. Morabito, C., et al., "Modulation of redox status and calcium handling by extremely low-frequency electromagnetic field in C2C12 muscle cells; a real time, single-cell approach," *FRBM*, Vol. 48, 579–589, 2010.
37. Hirose, E., et al., "A new 3-axis magnetic field measurement system based on hall elements," *IEEE Trans. on Applied Superconductivity*, Vol. 14, No. 2, 1814–1817, 2004.